[December, 1987] Bull. Chem. Soc. Jpn., 60, 4197—4201 (1987)

$AlBr_3$ Group Reorientation in $NaAl_2Br_7$ and KAl_2Br_7 Studied by Means of ^{81}Br, ^{27}Al NQR and ^{27}Al NMR

Koji Yamada,* Tsutomu Okuda, and Sumio Ichiba
Department of Chemistry, Faculty of Science, Hiroshima University, Naka-ku, Hiroshima 730
(Received February 27, 1987)

^{81}Br NQR spin-lattice relaxation times for MAl_2Br_7 (M=Na and K) were measured from 77 to 373 K and the reorientational activation energies of the $AlBr_3$ groups about Al-Br(bridge) axes were determined. In the case of $NaAl_2Br_7$, the reorientation of the $AlBr_3$ group was also confirmed by a motional narrowing effect of the ^{27}Al NMR using a single crystal. In order to examine the effect of the reorientation on the Al site, ^{27}Al NQR frequencies in $NaAl_2Br_7$ were observed as a function of temperature by a SEDOR technique. The asymmetry parameter (η) of the electric field gradient (efg) tensor was found to increase at one of the two Al sites with the onset of the reorientation.

NQR spin-lattice relaxation times (T_1) have been measured in order to study reorientation of molecules or molecular fragments[1,2] and also molecular motions in the vicinity of phase transitions.[3] This is due to the fact that the NQR relaxation rate increases because of the large fluctuation of its efg tensor induced by molecular motions. The dynamical properties of the compounds containing reorientationable groups such as $-CCl_3$, $-PCl_3$, and $=PCl_3$ have been studied by ^{35}Cl NQR T_1.[4-9] In contrast to proton NMR experiment in the solid state, the measurements of the NQR relaxation times give dynamical information at each crystallographically different site. This advantage was clearly shown for p-$CCl_3C_6H_4Cl$[4] and $AlBr_3 \cdot 2CH_3CN$ which has the ionic structure $AlBr(CH_3CN)_5{}^{2+} \cdot 2AlBr_4{}^- \cdot CH_3CN$.[10]

According to the crystal structures of KAl_2Br_7 and $NH_4Al_2Br_7$, the $Al_2Br_7{}^-$ anion consists of two $AlBr_4$ tetrahedra sharing one Br atom. The Al-Br-Al bridge angle is close to regular tetrahedral one and the two $AlBr_3$ groups are arranged in a staggered configuration to minimize halogen-halogen repulsions.[11,12] In our previous paper it was shown from the ^{27}Al NMR experiments, using a single crystal of KAl_2Br_7, that the angle between efg z-axes of the ^{27}Al was by about 9 degrees larger than that of ∠Al-Br-Al.[13] Similarly the angle between approximate C_3 axes of $AlBr_3$ groups, which were determined as a geometrical means of the three efg z-axes of the terminal Br atoms, is larger than ∠Al-Br-Al and almost consistent with the angle deduced from the ^{27}Al NMR. Accordingly, the approximate C_3 axis of the $AlBr_3$ group is not parallel to the Al-Br(bridge) direction and hence the bridging bond forms a "bent bond" or "banana bond" similar to the Al-Br-Al bond that occurs in the dimeric Al_2Br_6 molecule.[14,15] The steric hindrance of the two $AlBr_3$ groups seems to be the reason for the "bent bond." Therefore, these two $AlBr_3$ groups may affect each other in the activation process of their reorientations. In this paper we report the dynamical property of the two $AlBr_3$ groups in the $Al_2Br_7{}^-$ anion by means of ^{81}Br NQR and ^{27}Al NMR. Furthermore, the effect of the $AlBr_3$ reorientation on the ^{27}Al NQR parameters was investigated as a function of temperature.

Experimental

The compounds $NaAl_2Br_7$ and KAl_2Br_7 were obtained by crystallizing the molten mixture containing $AlBr_3$ and relevant alkali bromides by the Bridgman method. About 5% excess of $AlBr_3$ was added above the stoichiometric ratio because of the incongruent melting property of the compounds.[11,16]

The ^{81}Br NQR relaxation time T_1 was measured by the 90°-90° pulse method using a Matec pulse spectrometer. A typical pulse length for the 90° pulse was about 5 μs with a coil diameter of 12 mm. ^{27}Al and ^{23}Na NQR signals were detected by the ^{81}Br-^{27}Al and ^{81}Br-^{23}Na spin echo double resonance (SEDOR) method respectively, where a strong ^{81}Br NQR echo signal was monitored. The relative positions of the Br atoms within the anion were also determined, because the sensitivity of the SEDOR method depends upon the dipole-dipole interaction under study.[17] The experimental procedure has been described elsewhere.[18]

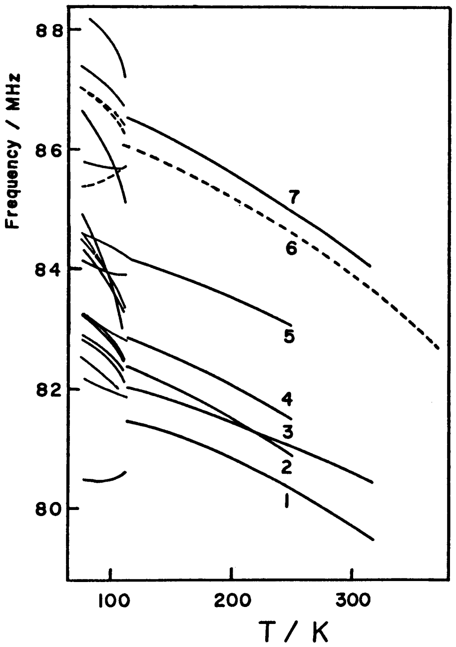

Fig. 1. Temperature dependence of the ^{81}Br NQR frequency in $NaAl_2Br_7$. The dotted curve Br(6) was assigned to the bridging atom.

Table 1. ^{27}Al and ^{23}Na NQR Parameters in $NaAl_2Br_7$ at Selected Temperature[a)]

Nucleus	Temp/K	Assignment[b)]	ν_1/MHz	ν_2/MHz	η	e^2Qqh^{-1}/MHz
^{27}Al	90	Al(1)′	1.306	2.561	0.039	8.692
		Al(1)′	1.356	2.696	0.068	8.995
		Al(1)′	1.370	2.735	0.037	9.120
		Al(2)′	1.460	2.767	0.213	9.285
		Al(2)′	1.482	2.869	0.161	9.611
		Al(2)′	1.522	2.982	0.127	9.972
	292	Al(1)	1.317	2.606	0.091	8.702
		Al(2)	1.456	2.873	0.102	9.598
^{23}Na	78		0.613, 0.493, 0.483			
	129		0.542			

a) Estimated error in ν is ±0.003 MHz. b) Below 113±1 K, Al(1) and Al(2) lines split into three lines Al(1)′ and Al(2)′ respectively.

Results and Discussion

$NaAl_2Br_7$. Figure 1 shows the temperature dependence of the ^{81}Br NQR frequencies. Above the phase transition temperature (T_c=113±1K) seven ^{81}Br NQR lines were observed as reported previously.[13)] Below T_c, however, the spectrum was very complicated and totally 21 ^{81}Br NQR lines could be detected suggesting three nonequivalent $NaAl_2Br_7$ units in the low temperature phase. This ^{81}Br NQR spectrum is consistent with ^{27}Al and ^{23}Na NQR spectra which have the six pairs of ν_1 (1/2↔3/2) and ν_2 (3/2↔5/2) and three lines respectively, as shown in Table 1. Above T_c two sets of three ^{81}Br NQR lines disappeared at about 250K and 320K respectively, but the remaining single line could be detected up to near the decomposition temperature of 370K. The relative positions of all the Br atoms in the $Al_2Br_7^-$ anion were determined by the SEDOR technique as described above. Then, the sets of three resonance lines which disappeared at almost the same temperatures could be assigned to the same $AlBr_3$ group and the remaining line to the bridging atom. There was no significant difference in the T_1 vs. temperature behavior among the three lines assigned to the same $AlBr_3$ group. Therefore, the temperature dependence of the ^{81}Br NQR spin-lattice relaxation times (T_1) were measured precisely only for three Br(1), Br (2), and Br (6) sites as shown in Fig. 2 together with their assignment. A small dip was observed near T_c for each line. The feature above 160 K is similar to that found in the compounds containing such reorientational groups as CCl_3 or PCl_3. The drastic decrease of the T_1 for Br (1) and Br (2) at high temperature may come from the $AlBr_3$ group reorientation about its approximate C_3 axis for the following reasons; (1) there was no significant difference in the T_1 vs. temperature curves which were assigned to the same $AlBr_3$ group, (2) the bridging atom Br (6) showed no drastic decrease of T_1 with temperature and (3) a line width transition of the ^{27}Al NMR was observed as described later. In this case the ^{81}Br NQR relaxation rate $(1/T_1)_{obs}$ may be described as a sum of the two mechanisms, lattice vibration $(1/T_1)_{vib}$ and reorientation of the $AlBr_3$ group $(1/T_1)_{reo}$ as follows,

$$\begin{aligned}(1/T_1)_{obs} &= (1/T_1)_{vib} + (1/T_1)_{reo}\\ &= a\,T^n + b\exp(-V/RT),\end{aligned} \qquad (1)$$

where V is the activation energy of the reorientation motion of the $AlBr_3$ group and the parameters a, n, and b are determined experimentally. Table 2 shows these parameters determined by a non-linear least squares method. Joes et al. showed that if the librational fluctuation governs the relaxation, n is equal to 2 for I=3/2 nuclei.[19)] The value of n obtained for the Br (1) is smaller than the theoretical one. This is probably due to the additional contribution to T_1 near the phase transition point, because the parameter n for the bridging Br (6) shows a value close to the theoretical one in the temperature range from 180 to 350K as shown in Table 2.

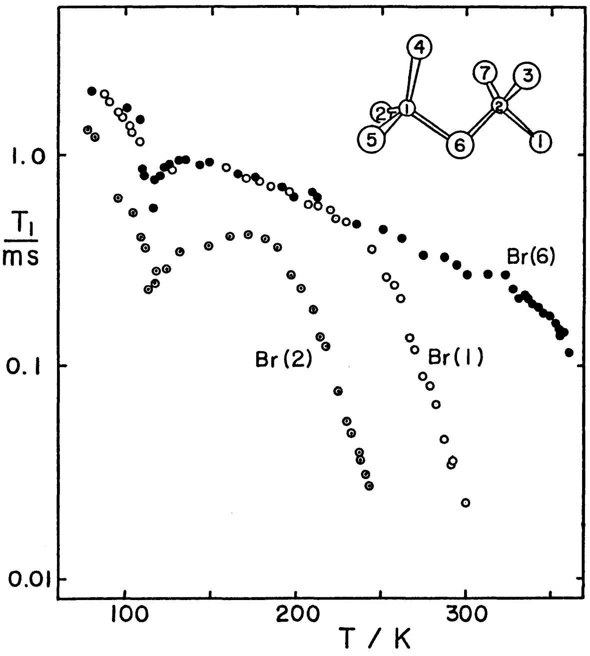

Fig. 2. Temperature dependence of the ^{81}Br NQR spin-lattice relaxation times T_1 in $NaAl_2Br_7$.

The $AlBr_3$ group reorientation could also be detected as a motional narrowing phenomena of the

Table 2. Best Fit Parameters of Eq. 1

Compound	Assignment	$a/10^{-2}$ s	n	$b/10^{12}$ s	V/kJ mol^{-1}	Temp/K
NaAl$_2$Br$_7$	Br(1), Al(2)Br$_3$	140.0	1.3	1.55	43.5	$171<T<300$
	Br(5), Al(1)Br$_3$			0.105	30.2	$182<T<243$
	Br(6), Brridge	2.9	2.1			$180<T<350$
KAl$_2$Br$_7$	Br(1), Al(1)Br$_3$	0.23	2.3	3470	81.4	$80<T<345$
	Br(2), Al(2)Br$_3$	0.26	2.2	5530	75.1	$80<T<368$

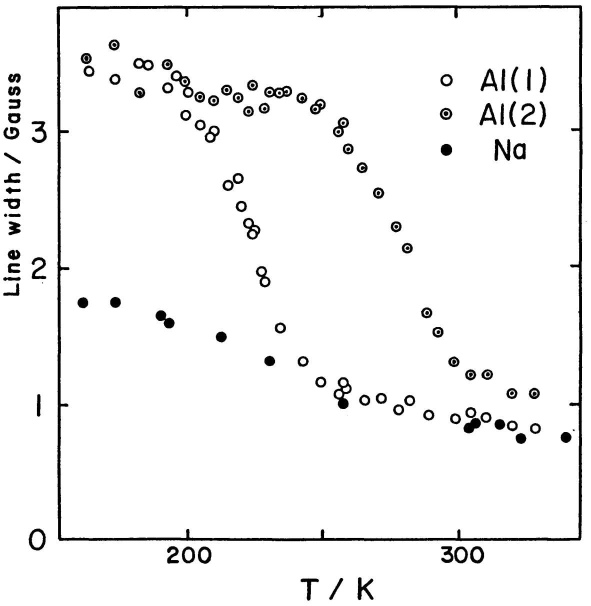

Fig. 3. ^{27}Al and ^{23}Na NMR line widths are plotted against temperature for NaAl$_2$Br$_7$ using single crystal.

^{27}Al NMR using a single crystal at 16 MHz. Figure 3 plots the line width against temperature together with that of the ^{23}Na NMR, where the line width is defined as the separation between the maximum and the minimum of the derivative curve. Because of the large quadrupole coupling constant at the Al site, central transitions ($-1/2 \leftrightarrow 1/2$) were shifted as a function of the crystal orientation with respect to the external magnetic field in terms of the second order quadrupole effect. Thus, the line width of the ^{27}Al NMR was observed at each site separately as a function of temperature. A precise analysis and assignment of the quadrupole splitting lines was reported previously.[13] Figure 4 shows a typical ^{27}Al NMR spectrum recorded at 271 K at a certain crystal orientation with respect to the external magnetic field, where Al (1) and Al (2) sites are in a motional narrowing and a rigid state in the NMR time scale, respectively. In general at the temperature where a line width transition takes places the following relation holds between the reorientational correlation time, τ_c, and the line width.

$$\tau_c = (1/H\alpha\gamma)\tan[\pi(H^2-B^2)/2(C^2-B^2)], \qquad (2)$$

where B, H, and C are the line width above, within and below the transition region respectively, γ is the gyromagnetic ratio and α is a numerical constant. On the other hand, the correlation time of the AlBr$_3$ reorientation is calculated from the $(T_1)_{\rm reo}$ data using a simple relation, $(T_1)_{\rm reo}=(3/4)\tau_c$.[20] The correlation times from the ^{81}Br NQR data are plotted against temperature in Fig. 5. If $\alpha=3.1\pm0.1$ is adopted as a numerical constant in Eq. 2 the correlation times from the ^{27}Al NMR agree well with those of the ^{81}Br NQR as shown in Fig. 5. This finding suggests that both the abrupt decrease in the NQR T_1 and the motional nar-

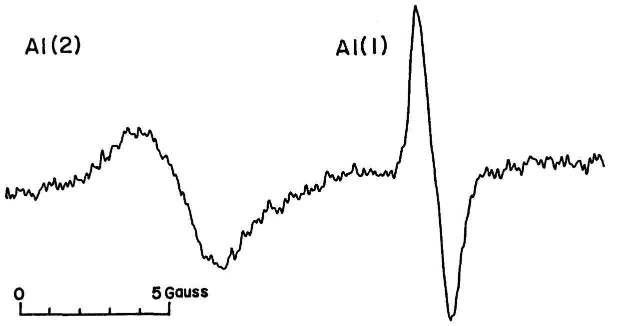

Fig. 4. Typical ^{27}Al NMR spectra for ($1/2 \leftrightarrow -1/2$) transitions at 271 K. A motional narrowing is completed for the Al(1) site at this temperature. The modulation width was chosen to be about 1/3 of each absorption line.

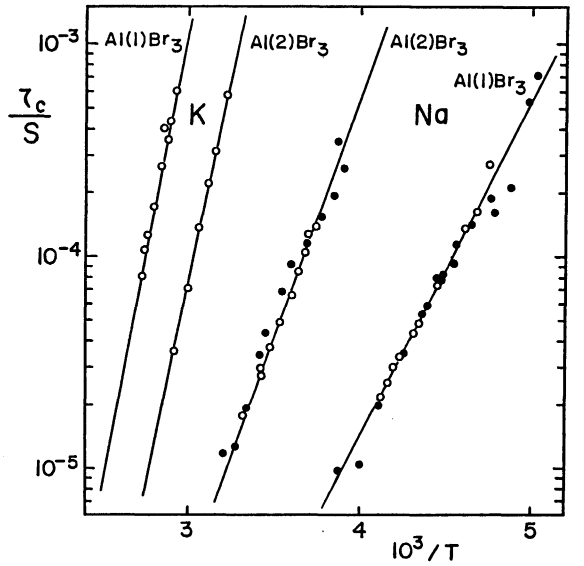

Fig. 5. Temperature dependence of the correlation times, τ_c, of the AlBr$_3$ reorientation for NaAl$_2$Br$_7$ and KAl$_2$Br$_7$. The lines were calculated from the second term of the Eq. 1 using the parameters in Table 1. ○: from ^{81}Br NQR T_1 data, ●: from ^{27}Al NMR line width data.

rowing of the ^{27}Al NMR are governed by the same mechanism, i.e., $AlBr_3$ reorientation about the C_3 axis.

In view of the low potential barrier of the $AlBr_3$ reorientation, the diffusion of the Na^+ cation was suspected to occur in the same manner as a Li^+ in $LiAlCl_4$.[21] The ^{23}Na line width was also measured as a function of temperature as shown in Fig. 3. Two central transitions ($-1/2\leftrightarrow1/2$) resulted from the monoclinic system were shifted by the second order quadrupole effect because of the large quadrupole coupling constant. The line width was observed at a certain orientation of the crystal where two central transitions separated from each other. The line width decreases from 1.8 to 0.8 Gauss. However, the narrowing limit of 0.8 Gauss is too large as a result of the diffusion and the narrowing temperature range is almost the same as that of the ^{27}Al NMR. Therefore, the ^{23}Na NMR narrowing probably results from the $AlBr_3$ groups reorientation and not from the diffusion of the Na^+ cation.

Figure 6 shows the temperature dependence of the ^{27}Al and ^{23}Na NQR frequencies above 113 K. The quadrupole coupling constants (e^2Qq/h) and asymmetry parameters (η) for the ^{27}Al are calculated using an exact formula for nuclear spin $I=5/2$[22] as is shown in Fig 7. If the reorientational frequency is much higher than that of NQR, the asymmetry parameter of the ^{27}Al reduces to zero due to the motional averaging of the $AlBr_3$ group. This is not the case, as is also expected from the temperature dependence of the correlation time in Fig. 5. However, it is interesting to note that at the Al (1) site the value of η increases with the onset of the $AlBr_3$ group reorientation. If the asymmetry parameter of the Al site is assumed to increase with the extent of the "bend bond" for the Al–Br (bridge) bond, the increase of the asymmetry parameter with the onset of the reorientation would be understandable because the activation energy for the reorientation is expected to decrease with the extent of the "bent bond."

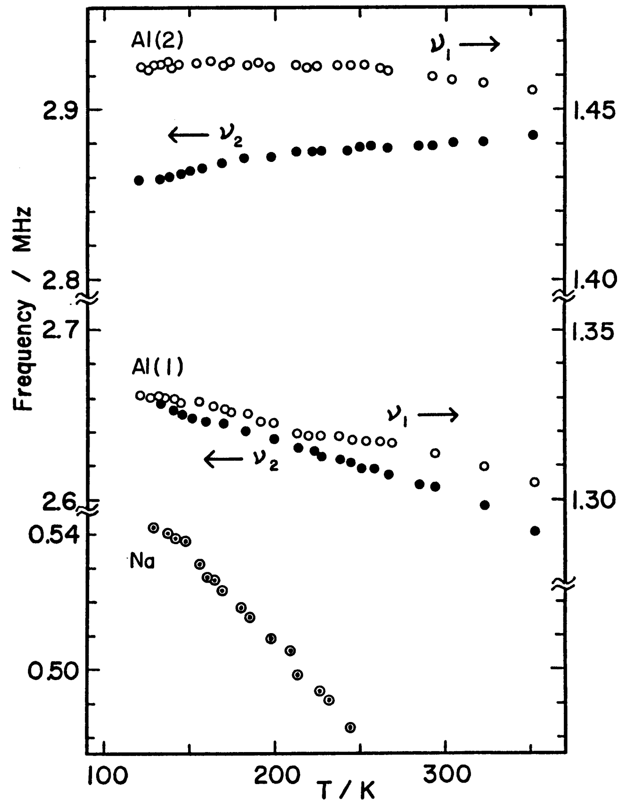

Fig. 6. Temperature dependence of the ^{27}Al and ^{23}Na NQR frequencies for $NaAl_2Br_7$. In the case of the ^{27}Al ν_1 and ν_2 correspond to ($1/2\leftrightarrow3/2$) and ($3/2\leftrightarrow5/2$) transitions, respectively.

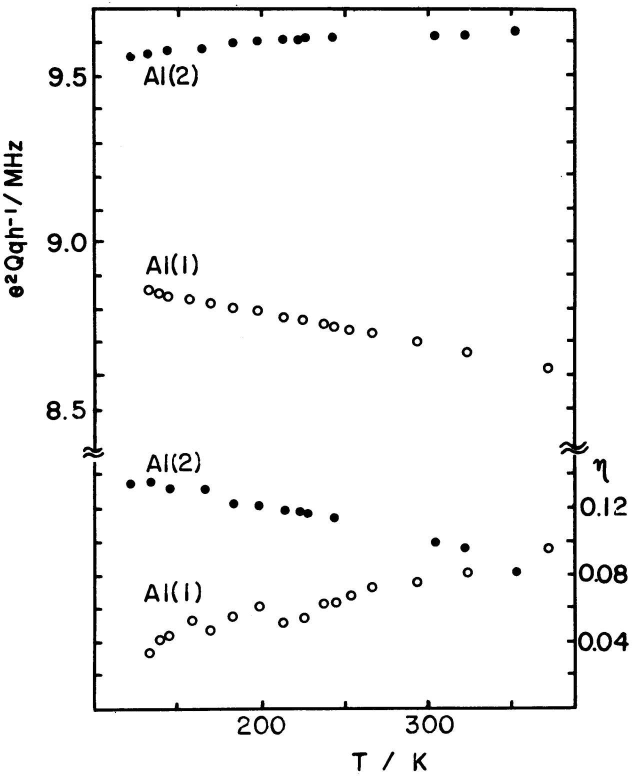

Fig. 7. Quadrupole coupling constant (e^2Qq/h) and asymmetry parameter (η) for the ^{27}Al NQR are plotted against temperature for $NaAl_2Br_7$.

KAl_2Br_7. The temperature dependence of the seven ^{81}Br NQR lines and their assignment for KAl_2Br_7 have been reported previously;[13,23] three lines belonging to the same $AlBr_3$ group disappeared at a temperature about 30 degrees below the decomposition temperature. Accordingly the reorientation of the $AlBr_3$ group was predicted from the fade out phenomena. Figure 8 shows the temperature dependence of the spin-lattice relaxation times for the ^{81}Br NQR lines which were assigned to the different $AlBr_3$ groups. Because of the overlapping of the NQR lines over the wide temperature range, the T_1 vs. temperature curve for the bridging Br could not be obtained. Table 1 shows the best fit parameters to Eq. 1. The values of b for these two sites are much larger than the values expected from the classical rotator approximation. A possible reason is the temperature dependency of the activation energy as suggested by the NMR experiment for ammonium sul-

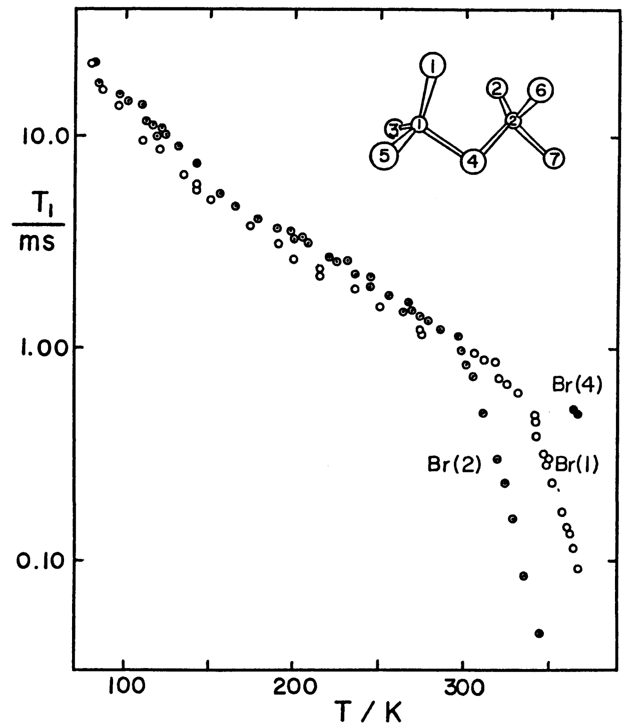

Fig. 8. Temperature dependence of the ^{81}Br NQR spin-lattice relaxation times T_1 in KAl$_2$Br$_7$.

fate.[24] For simplicity we assume that the activation energy V decreases linearly with increasing temperature as

$$V = V_0 - CT, \quad (3)$$

where V_0 is an activation energy extrapolated to 0 K and where C is a temperature coefficient. The Eq. 1 then becomes

$$1/T_1 = a\,T^n + 10^{12} \exp\left(-(V_0 - CT)/RT\right), \quad (4)$$

$$= a\,T^n + b_0 \exp\left(-V_0/RT\right), \quad (5)$$

where $b_0 = 10^{12} \exp(C/R)$. In these equations $b = 10^{12}$ s was assumed as a pre-exponent factor from the classical rotator model. Eq. 5 is the same as that of Eq. 1. Therefore, only from the measurements in the narrow temperature range is it impossible to deduce whether the activation energy has a temperature dependence or not. Using the values of Table 2 the temperature coefficient C were calculated to be 0.068 and 0.072 kJ mol^{-1} K^{-1} for the Br (1) and Br (2) sites, respectively. Accordingly activation energies fall down to about 70% of the values listed in Table 1, at the temperature where the NQR signals disappear. At present we have no other experimental evidence for the temperature dependence of the activation energy. However it may be reasonable because the two AlBr$_3$ groups have large steric repulsions and affect each other in the activation process of the reorientation.

References

1) H. Chihara and N. Nakamura, *Adv. Nucle. Quadrupole Reson.*, **4**, 1 (1981).

2) R. S. Lotfullin and G. K. Semin, *Adv. Nucle. Quadrupole Reson.*, **2**, 1 (1975).

3) R. L. Armstrong, *J. Magn. Reson.*, **20**, 214 (1975).

4) T. Kiichi, N. Nakamura, and H. Chihara, *J. Magn. Reson.*, **30**, 603 (1978).

5) Y. Yoshioka, N. Nakamura, and H. Chihara, *J. Mol. Struc.*, **111**, 195 (1983).

6) M. MaCkowski and M. Zdanowska, *Acta Phys. Pol.*, **A48**, 723 (1975).

7) I. V. Izmestyev, *Opt. Spectrosc.*, **30**, 557 (1971).

8) I. A. Kjunzel, V. A. Mokeeva, and G. B. Soifer, *Spectroscopy Lett.*, **8**, 113 (1975).

9) I. A. Kjunzel, V. A. Mokeeva, G. B. Soifer, and I. G. Shaposhinikov, *J. Magn. Reson.*, **20**, 394 (1975).

10) K. Yamada, T. Okuda, and H. Negita, *Z. Naturforsch.*, **41a**, 230 (1986).

11) E. Rytter, B. E. D. Rytter, H. A. ϕye, and J. Krogh-Moe, *Acta Crystallogr., Sect., B*, **29**, 1541 (1973).

12) E. Rytter, B. E. D. Rytter, H. A. ϕye, and J. Krogh-Moe, *Acta Crystallogr., Sect., B*, **31**, 2177 (1975).

13) K. Yamada, *J. Sci. Hiroshima Univ.*, **A41**, 77 (1977).

14) P. A. Casabella, P. J. Bray, and R. G. Barnes, *J. Chem. Phys.*, **30**, 1393 (1959).

15) T. Okuda, H. Terao, O. Ege, and H. Negita, *J. Chem. Phys.*, **52**, 5480 (1970).

16) C. T. H. M. Cronenberg and J. W. van Spronsen, *Z. Anorg. Allg. Chem.*, **354**, 103 (1967).

17) M. Emshwiller, E. L. Hahn, and D. Kaplan, *Phys. Rev.*, **118**, 414 (1960).

18) K. Yamada and T. Okuda, *J. Phys. Chem.*, **89**, 4269 (1985).

19) L. V. Jones, M. Sabir, and J. A. S. Smith, *J. Phys.*, **C11**, 4077 (1978).

20) S. Alexander and A. Tzalmona, *Phys. Rev.*, **A138**, 845 (1965).

21) W. Weppner and R. A. Huggins, *Phys. Lett.*, **58A**, 4, 245 (1976).

22) R. B. Creel, H. R. Brooker, and R. G. Barnes, *J. Magn. Reson.*, **41**, 146 (1980).

23) N. Weiden and A. Weiss, *J. Magn. Reson.*, **20**, 403 (1978).

24) D. E. O'Reilly and T. Tsang, *J. Chem. Phys.*, **46**, 1291 (1976).